Available online at www.sciencedirect.com
SCIENCE DIRECT®
Journal of Organometallic Chemistry 689 (2004) 3265–3274
Journal of Organometallic Chemistry
www.elsevier.com/locate/jorganchem

Reactivity studies of (η^6-arene)ruthenium dimeric complexes towards pyrazoles: isolation of amidines, bis pyrazoles and chloro bridged pyrazole complexes

P. Govindaswamy [a], Yurij A. Mozharivskyj [b], Mohan Rao Kollipara [a,*]

[a] *Department of Chemistry, North-Eastern Hill University, Shillong 793022, India*
[b] *Ames Laboratory, Iowa State University of Science and Technology, Ames, IA 50011, USA*

Received 8 June 2004; accepted 22 July 2004
Available online 24 August 2004

Abstract

The complex [(η^6-*p*-cymene)Ru(μ-Cl)Cl]$_2$ **1** reacts with pyrazole ligands (**3a–g**) in acetonitrile to afford the amidine derivatives of the type [(η^6-*p*-cymene)Ru(L)(3,5-HRR′pz)](BF4)$_2$ (**4a–f**), where L = {HN=C(Me)3,5-RR′pz}; R, R′ = H (**4a**); H, CH_3 (**4b**); C_6H_5 (**4c**); CH_3, C_6H_5 (**4d**) OCH_3 (**4e**); and OC_2H_5 (**4f**), respectively. The ligand **L** is generated in situ through the condensation of 3,5-HRR′pz with acetonitrile under the influence of [(η^6-*p*-cymene)RuCl$_2$]$_2$. The complex [(η^6-C_6Me_6)Ru(μ-Cl)Cl]$_2$ **2** reacts with pyrazole ligands in acetonitrile to yield bis-pyrazole derivatives such as [(η^6-C_6Me_6)Ru (3,5-HRR′pz)$_2$Cl](BF$_4$) (**5a–b**), where R, R′ = H (**5a**); H, CH_3 (**5b**), as well as dimeric complexes of pyrazole substituted chloro bridged derivatives [{(η^6-C_6Me_6)Ru(μ-Cl)(3,5-HRR′pz)}$_2$](BF$_4$)$_2$ (**5c–g**), where R, R′ = CH_3 (**5c**); C_6H_5 (**5d**); CH_3, C_6H_5 (**5e**); OCH_3 (**5f**); and OC_2H_5 (**5g**), respectively. These complexes were characterized by FT-IR and FT-NMR spectroscopy as well as analytical data. The molecular structures [1] of representative complexes [(η^6-C_6Me_6)Ru{3(5)-Hmpz}$_2$Cl]$^+$ **5b**, [(η^6-C_6Me_6)Ru(μ-Cl)(3,5-Hdmpz)]$_2^{2+}$ **5c** and [(η^6-C_6Me_6)Ru(μ-Cl){3(5)Me,5(3)Ph-Hpz}]$_2^{2+}$ **5e** were established by single crystal X-ray diffraction studies.

Keywords: *p*-Cymene; Hexamethylbenzene; Pyrazoles; Amidine; Ruthenium

1. Introduction

In recent years, the coordination chemistry of chelated ligands containing mixed functionalities on transition metal centers has been an extremely active area of research [1]. In particular, transition metal complexes with a coordination group, which is π electron bonded (like the cyclopentadienyl ligand) have attracted attention from the viewpoints of improving and elucidating catalytic processes such as olefin polymerization [2–5]. The η^6-arene ligands are isoelectronic with η^5-cyclopentadienyl ligands and the syntheses of η^6-arene complexes are much easier than that of cyclopentadienyl complexes. The three-legged piano stool structure of arene–ruthenium(II) complexes have attracted interest in recent years [6] due to their exhibition of catalytic [7] and anticancer activities [8]. Recently, a lot of interest has been given to these complexes due to the preparation of water-soluble arene–ruthenium complexes [9], which exhibit antibiotic, antiviral and catalytic activity such as the hydrogenation of bicarbonate in aqueous solution [9].

Reactions between free nitriles and nucleophiles such as amines, alcohols and water usually proceed in

* Corresponding author. Tel.: +91 364 272 2620; fax: +91 364 255 0076.
E-mail addresses: kmrao@nehu.ac.in, mrkollipara@yahoo.com (M.R. Kollipara).

[1] In the case of amidine, the molecular structure of representative complex was published in *J. Coordination Chem.* 56 (2003) 1085–1091.

0022-328X/$ - see front matter © 2004 Elsevier B.V. All rights reserved.
doi:10.1016/j.jorganchem.2004.07.036

presence of Lewis acid or base [10]. Ruthenium-containing η^5-cyclopentadienyl or η^6-benzene ligands have been the subject of active studies focusing on their use in organic synthesis [11]. However, arene–ruthenium compounds with coordinated nitriles react with the nucleophiles without the help of a Lewis acid or base [12] to form amidine complexes. McCleverty et al. [13] and we reported [14] the condensation of acetonitrile and pyrazole ligands bonded to an arene–ruthenium $[(\eta^6\text{-arene})RuCl_2]_2$ to form amidine complexes. Only a few other examples of formation of this type of amidine derivatives in transition metal complexes with coordinated nitriles have been reported [15]. During investigation of the reactivity studies of ruthenium(II) complex with nucleophiles, such as pyrazoles are inserted to the coordinated acetonitrile to give stable (η^6-arene)-ruthenium(II) amidine complexes of the form $[(\eta^6\text{-arene})Ru(L)(3,5\text{-}HRR'pz)][BF_4]_2$, where L = 1-methylcarbaldi- mino-3,5-subsituted pyrazoles.

Recently Faure et al. [16,17] reported the ability of the cluster cation $[H_3Ru_3(C_6H_6)\ (C_6Me_6)(O)]^+$ to efficiently catalyze the hydrogenation of benzene to give cyclohexane under biphasic conditions. In the search for new building blocks for the synthesis of arene–ruthenium clusters, we obtained mononuclear disubstituted and chloro-bridged pyrazole complexes. The reaction of complex **2** $[(\eta^6\text{-}C_6Me_6)Ru(\mu\text{-}Cl)Cl]_2$ with 3,5-disubstituted pyrazoles surprisingly yielded chloro bridged pyrazole complexes of the type $[(\eta^6\text{-}C_6Me_6)_2Ru_2(\mu\text{-}Cl)_2\text{-}(3,5\text{-}RR'pz)_2]$. To the best of our knowledge, only cleavage of both terminal and bridged chloride ligands has been reported so far [18].

Herein, we present the syntheses of the following arene–ruthenium complexes – the amidine complexes, the substituted bis(pyrazole) complexes and the chloro bridged pyrazole complexes. The single-crystal X-ray structure analyses of $[(\eta^6\text{-}C_6Me_6)Ru\{3(5)\text{-}Hmpz\}_2(Cl)]^+$, $[(\eta^6\text{-}C_6Me_6)_2Ru_2(\mu\text{-}Cl)_2(3,5\text{-}Hdmpz)_2]^{2+}$, and $[(\eta^6\text{-}C_6Me_6)Ru(\mu\text{-}Cl)\{3(5)\ Me,5(3)Ph\text{-}Hpz\}]_2^{2+}$ are reported as well.

2. Experimental

2.1. Physical measurements

Elemental analysis was performed in a Perkin–Elmer-2400 CHN/O analyzer. Infrared spectra were recorded on a Perkin–Elmer-model 983 spectrophotometer with the sample prepared as KBr pellets. Electronic spectra were recorded on a Hitachi-300 spectrophotometer. The ^1H NMR and ^{13}C $\{^1H\}$ NMR spectra were recorded in acetone-d_6 and $CDCl_3$ solvents with tetramethylsilane as internal standard and recorded on Bruker AMX-400 (400 MHz) and Bruker ACF-300 (300 MHz) spectrometers, the coupling constants J being given in Hz. Electrospray ionization mass spectra were obtained in positive-ion mode with a Shimadzu LCMS 2010 triple quadruple mass spectrometer.

2.2. Materials and methods

All chemicals used were of reagent grade. All reactions were carried out in distilled and dried solvents. $RuCl_3 \cdot 3H_2O$ was purchased from Arora Matthey Ltd., and used as received. The ligands such as pyrazole (Hpz) (**3a**) and 3-methylpyrazole (3-Hmpz) (**3b**) (from Merck) were used as received. The precursor complexes $[\{(\eta^6\text{-arene})Ru(\mu\text{-}Cl)Cl\}_2]$, {where η^6-arene = *p*-cymene (**1**) or hexamethylbenzene (**2**)} were prepared according to the literature procedures [19,20]. We adopted the literature procedure to synthesize the ligands [21].

2.3. Preparation of ligands

2.3.1. dimethylpyrazole (3,5-Hdmpz) (*3c*)

Acetylacetone (2 ml) and excess of hydrazine hydrate (~5 ml) were stirred for 15 min, whereby white solid precipitated out. The white solid was filtered and washed with hexane and dried under vacuum (yield 83.33%).

The same method was used for the preparation of other disubstituted pyrazoles taking the corresponding diketones instead of acetyl acetone. In the case of **3f** and **3g,** methanol (15 ml) was used as a solvent to dissolve the ketones (Table 1).

3. Preparation of compounds

3.1. $[(\eta^6\text{-}p\text{-}cymene)Ru(Hpz)(L)](BF_4)_2$ (*4a*) {L = HN=C(Me)pz}

The following general procedure was used to synthesize the complexes **4a–4f**.

A mixture of $[\{(\eta^6\text{-}p\text{-cymene})Ru(\mu\text{-}Cl)Cl\}_2]$ (0.163 mmol) and pyrazole ligand **3a–3g** (1.141 mmol) in acetonitrile (20 ml) were refluxed for 10–15 min, cooled to room temperature and filtered. The yellow filtrate was stirred for one hour and then NH_4BF_4 (1.141 mmol) was added and stirred again for 15 min. The solvent was removed under reduced pressure when an oily mass separated out. The oily mass was dissolved in dichloromethane and then filtered. The solution was concentrated to 2 ml and excess hexane was added for precipitation. The yellow compound was separated out and dried under vacuum.

4a: (Yield 52.56%). Elemental Anal. (%) for $C_{18}H_{25}RuN_5B_2F_8$: C, 38.88; H, 4.29; N, 11.94. Found: C, 38.36; H, 4.02; N, 12.02%. IR (KBr pellets, cm^{-1}): $\nu_{(N-H)}$ 3429 (s), 3104 (s) $\nu_{(amidine\ C=N)}$ 1646 (s), $\nu_{(pyrazole\ C-N)}$ 1527 (s), $\nu_{(B-F)}$ 1062 (s). ^1H NMR (acetone-d_6, δ): 1.11 & 1.23 (d, 6H, $CHMe_2$), 2.04 (s, 3H, CH_3), 2.75

Table 1
Ligand codes and IR data of ligands

Sl No.	Ligand		IR data (KBr pellets, cm^{-1}); $\nu_{(NH)}$ and $\nu_{(pyrazole\ C–N)}$
3c	3,5-Dimethylpyrazole	3,5-Hdmpz	3197 (m), 1593 (m)
3d	3,5-Dimethoxypyrazole	3,5-HdMeopz	3283 (m), 1606 (m)
3e	3,5-Diethoxypyrazole	3,5-HdEtopz	3264 (m), 1606 (m)
3f	3,5-Diphenylpyrazole	3,5-HdPhpz	3323 (m), 1600 (m)
3g	3(5)Methyl 5(3)-phenylpyrazole	3(5)Me,t 5(3)PhHpz	3325 (m), 1597 (m)

(sep, 1H, *CH*Me_2), 3.03 (s, 3H, CH_3), 6.05 (d, 2H, $J = 6.08$), 6.25 (d, 2H, $J = 6.04$), 6.58 (t, 1H, CH pz), 7.03 (t, 1H, CH pz), 7.80 (d, 1H, $J = 3.24$, CH pz), 8.71 (d, 1H, $J = 3.08$, CH pz), 8.91 (d, 1H, $J = 1.88$, CH pz), 9.28 (d, 1H, 1.86, CH pz), 11.9 (s, 1H, NH), 12.3 (s, 1H, NH). ^{13}C NMR (acetone-d_6, δ): 22.34, 23.14, 26.48,27.01 (CH_3), 33.67 [CH-(CH_3)$_2$], 86.32, 87.08, 89.31, 90.79 (CH, cymene), 92.67, 107.28 (C, cymene), 108.43, 110.61, 111.91, 112.89, 113.15 117.15 (pz), 156.23 (pz, NC–Me). UV–Vis (CH_2Cl_2): λ_{max} = 416 nm.

(4b) *[(η^6-p-cymene)Ru{3(5)-Hmpz}(L)](BF$_4$)$_2$ {L = HN=C(Me)mpz}*. (Yield 58.66%) Elemental Anal. (%) for $C_{20}H_{29}RuN_5B_2F_8$: C, 39.11; H, 4.75; N, 11.39. Found: C, 38.95; H, 4.36; N, 11.06%. IR (KBr pellets, cm^{-1}): $\nu_{(N–H)}$ 3317 (b), 3138 (s), $\nu_{(amidine\ C=N)}$ 1653 (m), $\nu_{(pyrazole\ C–N)}$ 1527 (m), $\nu_{(B–F)}$ 1076 (s). ^{1}H NMR (acetone-d_6, δ): 1.15 & 1.18(d, 6H, CH*Me$_2$*), 2.20 (sep, 1H, *CH*Me_2), 2.37 (s, 3H, CH_3), 2.47 (s, 3H, CH_3), 2.85 (s, 3H, CH_3), 3.20 (s, 3H, CH_3), 5.98 (d, 2H, $J = 6.12$), 6.20 (d, 2H, $J = 6.12$), 7.03 (d, 1H, $J = 3.12$, CH pz), 8.59 (d, 1H, $J = 3.12$, CH pz), 8.67 (d, 1H, $J = 3.08$, CH pz), 9.13 (d, 1H, $J = 2.00$, CH pz), 11.80 (s, 1H, NH), 12.23 (s, 1H, NH). ^{13}C NMR (acetone-d_6, δ): 15.08, 18.21, 20.42, 22.44, 24.96, 26.46 (CH_3), 33.59 [CH-(CH_3)$_2$], 86.94, 87.90, 88.29, 89.49 (CH, cymene), 91.76, 94.22(C, cymene), 112.38, 112.86, 117.35, 118.32, 140.15, 149.56 (pz), 155.51 (NC–Me). UV–Vis (CH_2Cl_2): λ_{max} = 419.3 nm.

(4c) *[(η^6-p-cymene)Ru(3,5-HdPhpz)(L)](BF$_4$)$_2$ {L = HN=C(Me)dPhpz}*. (Yield 56.94%) Elemental Anal. (%) for $C_{42}H_{41}RuN_5B_2F_8$: C, 56.65; H, 4.64; N, 7.86. Found: C, 56.33; H, 4.85; N, 7.53%. IR (KBr pellets, cm^{-1}): $\nu_{(N–H)}$ 3449 (s), 3177 (s), $\nu_{(amidine\ C=N)}$ 1653 (m), $\nu_{(pyrazole\ C–N)}$ 1566 (s), $\nu_{(B–F)}$ 1082 (s). ^{1}H NMR (acetone-d_6, δ): 1.08, & 1.12 (d, 6H, CH*Me$_2$*), 2.21 (s, 3H, CH_3), 2.30 (s, 3H, CH_3), 2.71 (sep, 1H, *CH*Me_2), 5.85 (d, 2H, $J = 6.13$), 6.01 (d, 2H, $J = 8.28$), 7.0–7.6 (m, 20H, Ph), 7.64 (s, 1H, CHpz), 7.90 (s, 1H, CH pz), 10.53 (s, 1H, NH), 11.13 (s, 1H, NH). ^{13}C NMR (acetone-d_6, δ): 17.89, 20.47, 21.28, 21.87 (CH_3), 28.99 (CH–Me_2), 79.95, 80.23, 82.14, 84.91 (CH, cymene), 87.46, 96.35 (C, cymene), 113.41, 125.29, 125.46, 125.78, 126.02, 126.34, 126.94, 127.82, 128.38, 128.75, 128.87, 128.94, 129.13, 129.47, 129.86, 130.09, 130.24, 130.87, 131.07, 131.78, 143.85, 148.40 (Ph, pz), 153.92 (NC–Me). UV–Vis (CH_2Cl_2): λ_{max} = 413 nm.

(4d) *[(η^6-p-cymene)Ru{3(5)Me, 5(3)Ph-Hpz}(L)](BF$_4$)$_2${L = HN=C(Me)Me, Phpz}*. (Yield 60.15%) Elemental Anal. (%) for $C_{32}H_{37}RuN_5B_2F_8$: C, 50.15; H, 4.86; N, 9.14. Found: C, 50.36; H, 5.64; N, 8.91%. IR (KBr pellets, cm^{-1}): $\nu_{(N–H)}$3423 (s), 3237 (s), $\nu_{(amidine\ C=N)}$1639 (s), $\nu_{(pyrazole\ C–N)}$ 1573 (m), $\nu_{(B–F)}$ 1082 (s). ^{1}H NMR (acetone-d_6, δ): 1.03 & 106 (d, 6H), 1.96 (s, 3H), 2.09 (s, 3H), 2.35 (s, 3H), 2.87 (sep, 1H), 3.03 (s, 3H), 6.26 (d, 2H, $J = 5.88$), 6.42 (s, 1H), 6.53 (d, 2H, $J = 5.92$), 6.77 (s, 1H), 7.21–7.84 (m, 10H), 11.51 (s, 1H), 11.76 (s, 1H). ^{13}C NMR (acetone-d_6, δ): 15.17, 18.34, 22.05, 22.39, 22.76, 29.14 (CH_3), 31.82 CH–Me_2, 80.24, 82.99, 84.19, 85.51 (CH, cymene), 88.79, 102.93 (C, cymene), 103.70, 106.97, 126.17, 126.58, 127.06, 127.97, 128.26, 128.92, 129.28, 129.85, 130.05, 131.54, 146.44, 149.18, (Ph, pz), 156.00 (NC–Me). UV–Vis (CH_2Cl_2): λ_{max} = 411 nm.

(4e) *[(η^6-p-cymene)Ru(3 5-HdMeopz)(L)](BF$_4$)$_2$ {L = HN=C(Me)Meopz}*. (Yield 55.26%). Elemental Anal. (%) for $C_{22}H_{33}RuO_4N_5B_2F_8$: C, 37.41; H, 4.71; N, 9.91. Found: C, 37.12; H, 4.93; N, 9.53%. IR (KBr pellets, cm^{-1}): $\nu_{(N–H)}$ 3449 (b), 3198 (s), $\nu_{(amidine\ C=N)}$1618 (s), $\nu_{(pyrazole\ C–N)}$ 1560 (s), $\nu_{(B–F)}$ 1083 (s). ^{1}H NMR (acetone-d_6, δ): 1.31 & 1.34(d, 6H, CH*Me$_2$*), 2.19 (s, 3H, CH_3), 2.82 (sep, 1H, *CH*Me_2), 3.18 (s, 3H, CH_3), 3.33 (s, 1H, CH_3), 3.41 (s, 1H, CH_3), 3.48 (s, 1H, CH_3), 3.58 (s, 1H, CH_3), 5.65 (d, 2H, $J = 5.80$), 5.76 (s, 1H CHpz), 5.88 (d, 2H, $J = 5.72$), 5.97 (s, 1H, CHpz), 9.22 (s, 1H, NH), 9.85 (s, 1H, NH). ^{13}C NMR (acetone-d_6, δ): 15.25, 18.32, 20.35, 26.91, 27.11, 27.28, 27.45, 28.42 (CH_3), 34.02 [CH(CH_3)$_2$, 84.37, 84.64, 85.31, 86.24 (CH, cymene), 89.12, 101.87 (C, cymene), 106.75, 111.96, 114.12, 116.97, 119.42, 122.56 (pz), 158.15 (NC–Me). UV–Vis (CH_2Cl_2): λ_{max} = 401 nm.

(4f) *[(η^6-p-cymene)Ru(3 5-HdEtopz)(L)](BF$_4$)$_2$ {L = HN=C(Me)Etopz}*. (Yield 56.87%). Elemental Anal. (%) for $C_{26}H_{41}RuN_5O_4B_2F_8$: C, 41.00; H, 5.42; N, 9.19. Found: C, 41.32; H, 4.97; N, 8.94%. IR (KBr pellets, cm^{-1}): $\nu_{(N–H)}$ 3448 (b), 3272 (s), $\nu_{(amidine\ C=N)}$ 1618(s), $\nu_{(pyrazole\ C–N)}$ 1560 (s), $\nu_{(B–F)}$ 1082 (s). ^{1}H NMR (acetone-d_6, δ): δ 1.32, & 1.35 (d, 6H, CH*Me$_2$*), 1.49 (s, 3H, CH_3), 2.18 (t, 3H, CH_3), 2.20 (t, 3H, CH_3), 2.22 (s, 3H, CH_3), 2.23 (t, 3H, CH_3), 2.29 (t, 3H, CH_3), 2.40 (sep, 1H *CH*Me_2), 3.34 (q, 2H, CH_2), 3.49 (q, 2H, CH_2), 3.53, (q, 2H, CH_2), 3.63 (q, 2H, CH_2), 5.73 (s, 1H, CHpz), 5.84 (s, 1H, CHpz), 5.98 (d,

2H, $J = 6.38$), 6.15 (d, 2H, $J = 6.12$), 9.01 (s, 1H, NH), 9.78 (s, 1H, NH). UV–Vis (CH_2Cl_2): $\lambda_{max} = 408$ nm.

3.2. *[(η⁶-C₆Me₆)Ru(Hpz)₂(Cl)]BF₄ (**5a**)*

The following general procedure was used to synthesize the complexes **5a**–**5g**.

A mixture of [{(η⁶-C_6Me_6)Ru(μ-Cl)Cl}$_2$] (0.149 mmol), pyrazole ligand (1.047 mmol) and NH_4BF_4 (1.047 mmol) were refluxed in acetonitrile (20 ml) for 30 min, cooled to room temperature and then filtered for removing NH_4Cl. The yellow filtrate was concentrated under reduced pressure. The oily mass was dissolved in dichloro-methane and filtered. The filtrate was concentrated to 2 ml and excess of hexane was added for precipitation. The yellow compounds were centrifuged and dried under vacuum.

5a: (Yield 58.13%). Elemental Anal. (%) for $C_{18}H_{26}RuN_4ClBF_4$: C, 41.43; H, 5.02; N, 10.73. Found: C, 41.71; H, 4.89; N, 10.57%. IR (KBr pellets, cm^{-1}): $\nu_{(N-H)}$ 3138 (s), $\nu_{(pyrazole\ C-N)}$ 1527 (s), $\nu_{(B-F)}$ 1082 (s). ^1H NMR ($CDCl_3$, δ): 2.06 (s, 18H, HMB), 6.74 (t, 2H), 6.41 (d, 2H, $J = 3.12$), 8.07 (d, 2H, 3.23), 11.70 (s, 2H, NH). UV–Vis (CH_2Cl_2): $\lambda_{max} = 407.4$ nm.

5b *[(η⁶-C_6Me_6)Ru{3(5)-Hmpz}$_2$(Cl)]BF_4*. (Yield 52.54%). Elemental Anal. (%) for $C_{20}H_{30}RuN_4ClBF_4$: C, 44.01; H, 4.80; N, 10.26. Found: C, 44.41; H, 4.58; N, 10.13%. IR (KBr pellets, cm^{-1}): $\nu_{(N-H)}$ 3283 (s), $\nu_{(pyrazole\ C-N)}$ 1573 (s), $\nu_{(B-F)}$ 1069 (s). ^1H NMR (acetone-d_6, δ): 2.08 (s, 18H, HMB), 2.82 (s, 6H, CH_3); 6.27 (d, 2H, $J = 2.87$, CHpz), 7.89 (d, 2H, $J = 3.04$, CHpz), 11.83 (NH, 2H). UV–Vis (CH_2Cl_2): $\lambda_{max} = 439.9$ nm.

5c*[(η⁶-C_6Me_6)Ru(μ-Cl)(3,5-Hdmpz)]$_2$(BF_4)$_2$*. (Yield 60.03%). Elemental Anal. (%) for $C_{34}H_{52}Ru_2N_5Cl_2B_2F_8$: C, 42.38; H, 5.44; N, 5.81. Found: C, 42.11; H, 5.62; N, 5.72%. IR (KBr pellets, cm^{-1}): $\nu_{(N-H)}$ 3204 (s), $\nu_{(pyrazole\ C-N)}$ 1573 (m), $\nu_{(B-F)}$ 1082 (s). ^1H NMR ($CDCl_3$, δ): 2.20 (s, 36H, HMB), 2.82 (s, CH3, 6H), 2.90 (s, CH3, 6H), 6.35 (s, 2H, CHpz), 11.42 (NH, 2H). MS (ESI): *m/z* 877 (M^+). UV–Vis (CH_2Cl_2): $\lambda_{max} = 416.10$ nm.

5d*[(η⁶-C_6Me_6)Ru(μ-Cl)(3, 5-HdPhpz)]$_2$(BF_4)$_2$*. (Yield 54.23%) Elemental Anal. (%) for $C_{54}H_{60}Ru_2N_4Cl_2B_2F_8$: C, 53.52; H, 4.99; N, 4.62. Found: C, 53.95; H, 5.02; N, 4.68%. IR (KBr pellets, cm^{-1}): $\nu_{(N-H)}$ 3197 (s), $\nu_{(pyrazole\ C-N)}$ 1566 (s), $\nu_{(B-F)}$ 1082 (s). ^1H NMR (acetone-d_6, δ): 2.80 (s, 36H, HMB), 5.29 (s, 2H, CHpz), 8.24–7.09 (m, 20H, Ph), 11.78 (NH, 2H). UV–Vis (CH_2Cl_2): $\lambda_{max} = 417.93$ nm.

5e *[(η⁶-C_6Me_6)Ru(μ-Cl){3(5)Me, 5(3)Ph-Hpz}]$_2$(BF_4)$_2$*. (Yield 57.14%). Elemental Anal. (%) for $C_{44}H_{56}Ru_2N_4Cl_2B_2F_8$: C, 48.59; H, 5.19; N, 5.15. Found: C, 48.64; H, 5.39; N, 5.25%. IR (KBr pellets, cm^{-1}): $\nu_{(N-H)}$ 3302 (s), $\nu_{(pyrazole\ C-N)}$ 1573 (m), $\nu_{(B-F)}$ 1082 (s). ^1H NMR ($CDCl_3$, δ): 2.51 (s, 6H, CH3), 2.79 (s, 36H, HMB), 6.41 (s, 2H, CHpz), 7.37–7.38 (m, 10H, Ph), 11.79 (s, 2H, NH). UV–Vis (CH_2Cl_2): $\lambda_{max} = 317$ nm.

5f*[(η⁶-C_6Me_6)Ru(μ-Cl)(3,5-HdMeopz)]$_2$(BF_4)$_2$*. (Yield 57.36%). Elemental Anal. (%) for $C_{34}H_{52}Ru_2N_4O_4Cl_2B_2F_8$: C, 39.74; H, 5.10; N, 5.45. Found: C, 39.55; H, 5.31; N, 5.68%. IR (KBr pellets, cm^{-1}): $\nu_{(N-H)}$ 3211 (s), $\nu_{(pyrazole\ C-N)}$ 1540 (m), $\nu_{(B-F)}$ 1082 (s). ^1H NMR ($CDCl_3$,δ): 2.10 (s, 36H, HMB), 3.82 (s, 6H, CH3), 3.42 (s, 6H, CH3), 5.46 (s, 2H, CHpz), 10.18 (s, 2H, NH). UV–Vis (CH_2Cl_2): $\lambda_{max} = 398$ nm.

5g *[(η⁶-C_6Me_6)Ru(μ-Cl)(3, 5-HdEtopz)]$_2$(BF_4)$_2$*. (Yield 53.69%). Elemental Anal. (%) for $C_{38}H_{60}Ru_2N_4O_4Cl_2B_2F_8$: C, 42.12; H, 5.58; N, 5.17. Found: C, 42.28; H, 5.42; N, 5.31%. IR (KBr pellets, cm^{-1}): $\nu_{(N-H)}$ 3230 (b), $\nu_{(pyrazole\ C-N)}$ 1543 (m), $\nu_{(B-F)}$ 1082 (s). ^1H NMR ($CDCl_3$, δ): 2.12 (s, 36H, HMB), 1.88 (t, 6H, CH_3), 1.98 (t, 6H, CH_3), 3.25 (q, 4H, CH_2), 3.49 (q, 4H, CH_2), 5.48 (s, 2H, CHpz), 9.57 (b, 2H, NH). UV–Vis (CH_2Cl_2): $\lambda_{max} = 398$ nm.

4. Crystallographic investigations

The single-crystal structure analysis of amidine complex [(η⁶-*p*-cymene)Ru{HN=C(Me)3,5-dmpz}(3,5-Hdmpz)]$^{2+}$ has been published previously [14] by us. X-ray quality crystals of the complexes **5b** and **5c** were grown by slow diffusion of hexane into dichloromethane solution and the complex **5e** was grown in $CDCl_3$ solution. A yellow crystal of complex **5b** and an orange crystals of complex **5c** and **5e** were mounted on a Bruker Apex CCD diffractometer in a full reciprocal sphere equipped with CCD detector and used for data collection. X-ray intensity data were collected with graphite monochromated Mo Kα radiation at 293(2) K, with 0.3° scans in ω scan in mode and 10 s per frame. The intensity data were corrected for Lorentz and polarization effects. The absorption correction was done using the SAINT program [22]. A summary of crystal data, data collection parameters and convergence results is compiled in Table 2. An empirical absorption correction was made by modeling a transmission surface by spherical harmonics employing equivalent reflections with $I > 3\sigma(I)$ (program SADABS) [23]. The structure was solved by direct methods [24]. All the non-hydrogen atoms were refined anisotropically using the full-matrix, least-squares technique on F^2 using the SHELXL-97 software [25]. All the hydrogen atoms were found from difference Fourier synthesis after four cycles of anisotropic refinement and as the "riding" model. Figs. 1–4 are the ORTEP [26] representations of the molecules with 50% (Fig. 1 is 30%) probability thermal ellipsoids displayed. Refinement converged at final R_1 values of 0.0546, 0.0564 and 0.0480 (for observed data *F*) for **5b**, **5c** and **5e**, respectively.

Table 2
Crystal data and structure refinement for complexes **5b**, **5c** and **5e**

Formula	$C_{20}H_{30}BClF_4N_4Ru$	$C_{34}H_{52}B_2Cl_2F_8N_4Ru_2$	$C_{44}H_{48}B_2Cl_2F_8N_4Ru_2$
M_r	549.81	963.46	1079.52
T (K)	293 (2)	293 (2)	293 (2)
Wavelength (Å)	0.71073	0.71073	0.71073
Crystal system	Monoclinic	Monoclinic	Triclinic
Space group	$P2_1/c$	$P2_1/n$	$P\bar{1}$
Unit cell dimensions			
a (Å)	9.8188(5)	9.5865(7)	10.3196 (17)
b (Å)	13.7982(7)	14.6210(11)	14.823 (3)
c (Å)	17.8018(9)	14.4797(11)	15.199 (3)
α (°)	90	90	86.838(3)
β (°)	102.543 (1)	94.313 (1)	81.107 (3)
γ (°)	90	90	84.585(3)
V (Å) ^{3}	2354.3(2)	2023.8(3)	2284.8(7)
Z	4	4	2
Crystal size (mm^3)	$0.12 \times 0.09 \times 0.08$	$0.3 \times 0.2 \times 0.2$	$0.06 \times 0.05 \times 0.03$
D_{calc} (g cm^{-3})	1.551	1.581	1.569
F(000)	1120	976	1088
θ (°)	1.88–28.27.	1.98–28.26.	1.38–17.57.
Reflections collected	20 154	17 308	7398
Independent reflections	5532 [R_{int} = 0.0232]	4748 [R_{int} = 0.0346]	2910 [R_{int} = 0.0431]
Completeness to θ	28.27°–94.8%	28.26°–94.6%	17.57°–99.2%
μ (Mo K α) (mm^{-1})	0.825	0.945	0.847
Data/parameters	5532/0/274	4748/0/223	2910/0/505
Goodness-of-fit on F^2	1.065	1.022	1.068
$R_1(I > 2I)$, wR_2	0.0546, 0.1571	0.0564, 0.1411	0.0466, 0.1149
R_1, R_2 (all data)	0.0615, 0.1647	0.0754, 0.1531	0.0713, 0.1332
Largest different peak and hole (e Å^{-3})	1.636 and −0.914	0.967 and −0.890	0.840 and −0.383

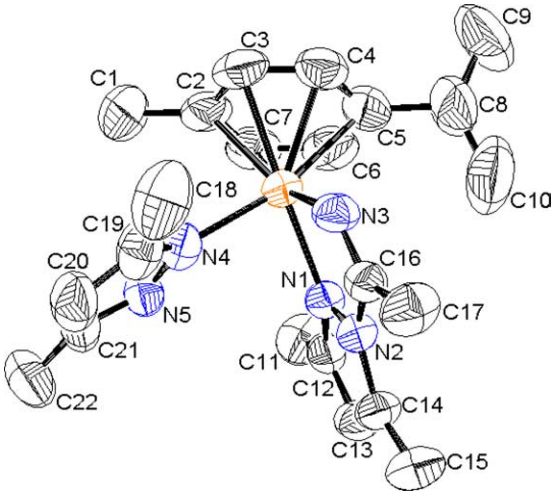

Fig. 1. ORTEP diagram[14] of complex [(η^6-*p*-cymene)Ru{NH=C(Me)3,5-dmpz}(3,5-Hdmpz)]$(BF_4)_2 \cdot H_2O$ with 30% probability thermal ellipsoids. Hydrogens and BF_4 are omitted for clarity of the figure. Selected bond lengths (Å) and bond angles (°). Bond lengths (Å): Ru(1)–N(4) 2.132(6); Ru(1)–N(1) 2.092(5); Ru(1)–N(3) 2.045(6); N(3)–C(16) 1.262(7); N(1)–N(2) 1.382(7); N(2)–C(16) 1.389(7). Bond angles (°): N(1)–Ru(1)–N(4) 83.6(2); N(3)–Ru(1)–N(4) 87.5(2); N(3)–Ru(1)–N(1) 74.3(2).

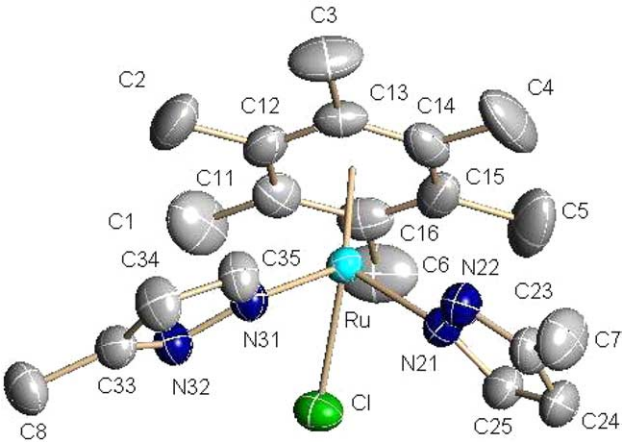

Fig. 2. ORTEP diagram of the complex **5b** with 50% probability thermal ellipsoids. Hydrogens and BF_4 are omitted for clarity of the figure. Selected bond lengths (Å) and bond angles (°). Bond lengths (Å): Ru–N(21) 2.116(3); Ru–N(31) 2.123(3); Ru–Cl 2.3979(10); N(31)–N(32) 1.338(5); N(31)–C(35) 1.328(5); N(21)–N(22) 1.366(5); N(21)–C(25) 1.326(5); Ru–C*1.685 *Ruthenium to centroid of HMB. Bond angles (°): N(31)–Ru–N(21) 88.06(13); N(31)–Ru–Cl 85.34(9); N(21)–Ru–Cl 85.8 (1).

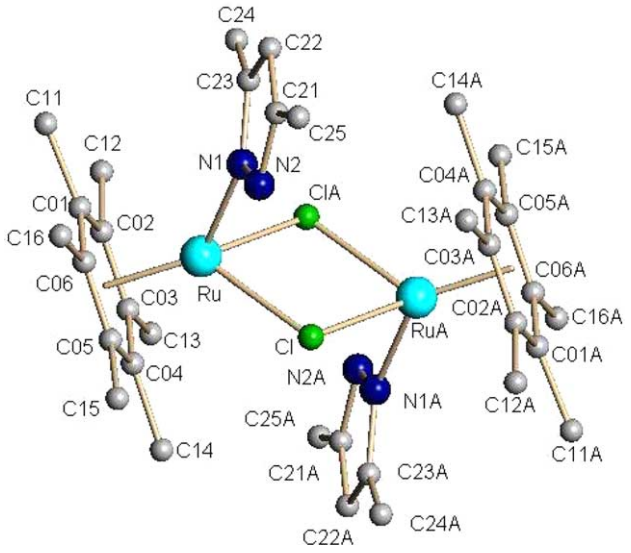

Fig. 3. Molecular structure of the complex **5c**. All the hydrogens and BF_4 are omitted for clarity of the figure. Selected bond lengths (Å) and bond angles (°). Bond lengths (Å): Ru–N(1) 2.107(2); Ru–Cl (A) 2.4475(12); Ru–Cl 2.4390(12); N(1)–C(23) 1.4200; N(1)–N(2) 1.4200; Ru–C* 1.684 *Ruthenium to centroid of HMB. Bond angles (°): N(1)–Ru–Cl 86.47(9) N(1)–Ru–Cl(A) 87.44(9) Cl–Ru–Cl(A) 80.82(4) Ru–Cl–Ru(A) 99.18(4).

5. Results and discussion

5.1. Preparation of ligands

The ligands **3c**–**3g** were synthesized by condensation of representative diketones with excess of hydrazine hydrate to afford 3,5-disubstituted pyrazole ligands (Scheme 1). The IR spectra of these ligands (Table 1) show strong bands in the range 3325–3197 cm^{-1} due to the ν_{N-H} group of the ligands and strong bands at around 1600 cm^{-1} due to the ν_{C-N} of the pyrazoles.

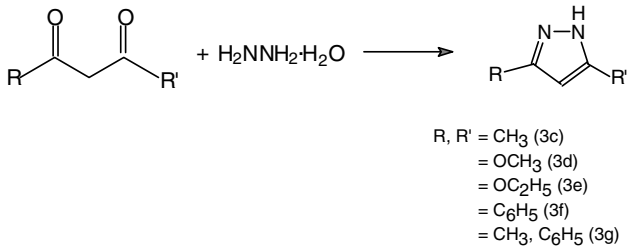

Scheme 1.

5.2. Amidine complexes

The reaction of complex **1** with an excess of substituted pyrazole ligands **3** in acetonitrile, followed by addition of NH_4BF_4, resulted the formation of yellow colored and air-stable complexes of the type **4** (Scheme 2) by the chloride bridge cleavage of complex **1**. In these complexes, the ruthenium atom is coordinated to *p*-cymene, which occupies three coordinate sites, the rest being occupied by the nitrogen's of amidine and pyrazole. The overall complex shows the piano-stool structure [27] (Fig. 1). The micro-analytical data suggested that the air-stable complexes obtained have the composition $[(\eta^6\text{-}p\text{-cymene})Ru\{HN{=}C(Me)(3,5\text{-}RR'pz)\}(3,5\text{-}HRR'\ pz)](BF_4)_2$. The in situ formation of the ligand 1-methylcarbaldimino-3,5-substituted pyrazole presumably takes place by condensation of 3,5-substituted pyrazole with acetonitrile, as activated by the complex **1**.

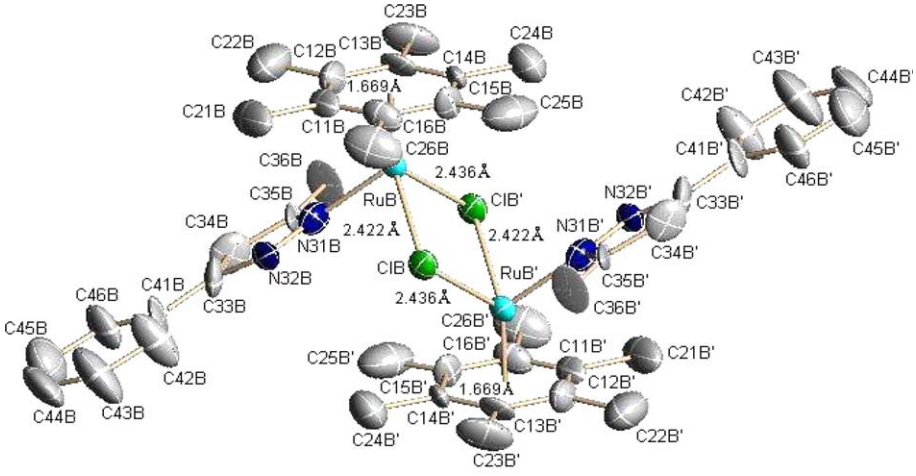

Fig. 4. ORTEP diagram of the complex **5e** (isomer B) with 50% probability thermal ellipsoids. Hydrogens and BF_4 are omitted for clarity of the figure. Selected bond lengths (Å) and bond angles (°). Bond lengths (Å): Ru(B)–C* 1.669 Ru(B)–N(31B) 2.103(7); Ru(B)–Cl(B) 2.423(3); Ru(B)–Cl(B′) 2.436(3); N(31B)–C(35B) 1.4200; N(31B)–N(32B) 1.4200 *Ruthenium to centroid of HMB. Bond angles (°): N(31B)–Ru(B)–Cl(B) 85.5(2); N(31B)–Ru(B)–Cl(B′) 88.2(2); Cl(B)–Ru(B)–Cl(B′) 81.18(11).

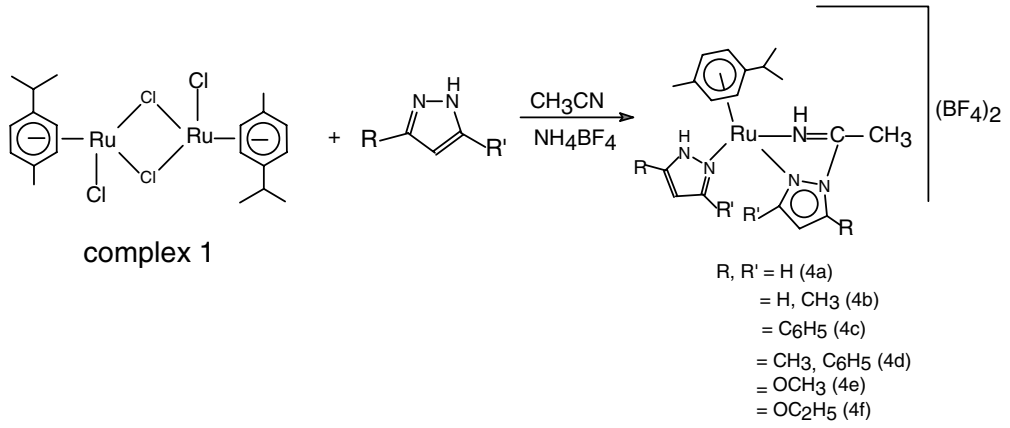

Scheme 2.

The formation of the amidine complex is confirmed by the appearance of the $\nu_{(\text{amidine C–N})}$ band in the range around 1653–1618 cm^{-1} of the IR spectrum. The ^1H NMR spectra of the complexes (**4a**–**f**) exhibit doublets for the methyl protons of the isopropyl group due to diasteriotopic nature of isopropyl group because ruthenium is at chiral center due to attachment four different ligands. A septet at the range 2.5–3 ppm is observed for the isopropyl proton. The two doublets observed at 5–6 ppm correspond to the aromatic *p*-cymene ring CH protons. The NH protons of amidine and the substituted pyrazole ligands give peaks in the range 9.01–12.30 ppm. The ^{13}C $\{^1H\}$ NMR spectrum also exhibits appropriate signals. The methyl carbons exhibit signals in the ranges between 15 and 30 ppm. The methyl carbons of the isopropyl group appear around 29–34 ppm, while the cymene carbons appear in the ranges between 82 and 107 ppm. The carbons of the arene group are thus similar to those in other similar reported compounds [28]. The carbons of the pyrazole and phenyl groups (CH, C-RR′, Ph) give peaks in the range 103–149 ppm, while, the C-atom of the incorporated acetonitrile, N*C*-Me appears at around 153–158 ppm. We had earlier confirmed the final structure of a representative complex of this kind through X-ray crystal studies [14]. The electronic spectra of complexes **4** in dichloromethane feature a UV–Vis pattern similar to that seen for the analogous Ru^{II} polypyridyl complexes [29] and arising from the metal–to–ligand charge transfer. The $Ru^{II}(d\ t_{2g})$ to ligand π^* transition appears at around 401–420 nm.

5.3. Monomeric complexes

The reaction of complex **2** with an excess of pyrazole **3a** and the 3,5-dimethyl-pyrazole ligand **3b** in acetonitrile gave the mononuclear complexes **5a** and **5b** (Scheme 3). The formation of these complexes **5a** and **5b** were conveniently monitored by the peak ratio in the ^1H NMR spectra and by elemental analyses. The infrared spectra of these complexes show a strong band in the range of 3283–3138 cm^{-1} due to the ν_{N-H} mode of the pyrazole ligands [30]. In addition, the IR spectra contain strong bands at 1573–1527 cm^{-1} due to the ν_{C-N} mode of the pyrazole ligands, and a strong band at 1082 cm^{-1} due to the ν_{B-F} mode of the BF_4 group. The ^1H NMR spectra of these complexes exhibit a strong peak at 2.06–2.08 ppm for hexamethylbenzene, which is slightly shifted downfield in comparison to the starting complex **2**, which exhibits it at 2.02 ppm. The resonance of the N–H proton of the pyrazole ligands is observed as a singlet in the range 11.70–11.83 ppm in these complexes. The complex **5a** exhibits two doublets at 6.41 and 8.07 ppm, and one triplet at 6.74 ppm due to the protons of the coordinated pyrazole ligand. The complex **5b** exhibits two doublets at 7.89 and 6.27 ppm, respectively, for the ring protons of pyrazole and one singlet at 2.82 ppm for the methyl group. The electronic spectra of these complexes in dichloromethane exhibit bands at 407 and 440 nm. These low-energy absorptions are assigned to the Ru^{II} $(d\pi)$ to ligand (π^*) metal-to-ligand charge transfer (MLCT) transition. The structure of the complex **5b** is shown in Fig. 2.

5.4. Chloro bridged pyrazole complexes

The reaction of the complex **2** with 3,5-disubstituted pyrazole ligands (**3c**–**g**) in acetonitrile resulted in the formation of yellow colored and air-stable dimeric chloro bridged pyrazole complexes of the type **5c**–**g** (Scheme 3) by substitution of the terminal chloride ligand. The similar reaction in the case of complex **1** invariably yielded amidine complexes. When using 3,5-disubstituted pyrazole ligands, only terminal N-coordinated pyrazole complexes are formed with the bridged chloride ligands instead of the expected monomeric or amidine

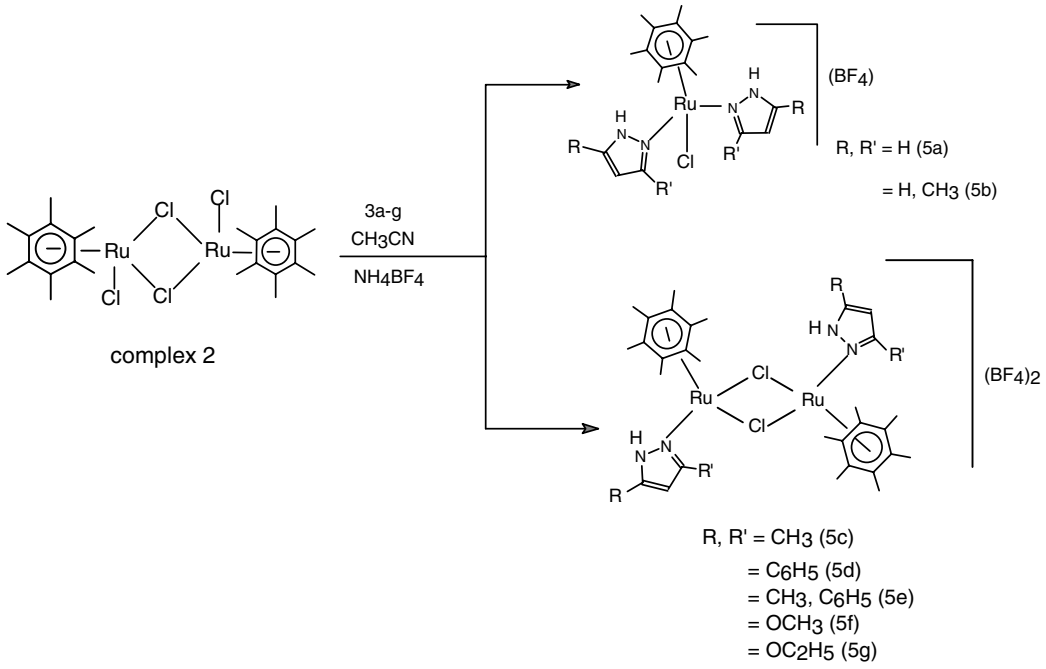

Scheme 3.

compounds. This suggests that bridged chloride ligands of complex **2** are cleaved in the first step, either by acetonitrile or by the pyrazole. Evidently for complexes (**5c**–**g**), coordination of the second pyrazole in the presumed monomeric intermediate $[RuCl_2(arene)(pz)]^+$ is slow compared with re-formation of the chloro bridge, possibly because of the greater steric bulk and electron-donating ability of C_6Me_6 relative to those of *p*-cymene. The formation of complexes **5c**–**g** is conformed by peak integration on the ^1H NMR spectra. The IR spectra of chloro bridged pyrazole complexes show a strong band at around 1573–1540 cm^{-1} due to ν_{C-N} mode present in the coordinated pyrazole ligands.

The ^1H NMR spectra of complexes **5c**–**g** display a sharp singlet for the methyl protons of hexamethylbenzene at around 2.1–2.8 ppm, while the peaks for the ligand moiety of the CH of pyrazole group appear in the range of 5.3–6.4 ppm. The NH proton of these complexes exhibits at around 9.6–11.8 ppm. The mass spectrum of the representative complex **5c** exhibits a molecular ion peak at around 877 (M^+). This molecular ion peak suggests that the complex is dimeric even in solution. Steric factors play a major role instead of electronic factors in the formation of these complexes. The bulky group ligands such as HMB and 3,5-disubstituted pyrazole ligands exert steric constraints to form these types of complexes instead of complexes of the type **5a**–**b** or **4a**–**f**. The electronic spectra of these complexes in dichloromethane exhibits bands in the range of 317–418 nm due to the Ru ($d\pi$) to ligand (π^*) metal-to-ligand charge transfer (MLCT) transition. The ORTEP diagrams of the complexes **5c** and **5e** are shown in Figs. 3 and 4, respectively.

6. Molecular structures

The single-crystal structure of the corresponding amidine complex (Fig. 1) has been published previously [14]. Single crystal X-ray structure determinations were carried out for complexes **5b**, **5c** and **5e** for confirmation of the formulation. Crystals of complexes **5b** and **5c** were grown by slow diffusion of hexane into dichloromethane, while complex **5e** was grown from dueterated chloroform solution. The ruthenium atom is coordinated to two molecules of the 3-methylpyrazole ligand through its ring nitrogen atom, one chloride ligand and one HMB molecule through η^6 fashion in the complex **5b**, whereas in the cases of complex **5c** and **5e,** each ruthenium atom is coordinated to two bridged chloride ligands, one nitrogen atom of 3,5-dimethylpyrzole, 3(5)methyl-5(3)-phenylpyrazole ligands and one molecule of hexamethylbenzene ligand. The geometry around the metal atom can be regarded as distorted octahedral if the η^6-hexamethyl–benzene group is assumed to occupy three facial coordinated positions.

The complex $[(\eta^6\text{-}C_6Me_6)Ru\{3(5)\text{-}Hmpz\}_2Cl]BF_4$ **5b** crystallizes in the monoclinic space group $P2_1/c$ (Fig. 2). In HMB, three of the Ru–C bond lengths, viz., those involving the C(11), C(13) and (16) are longer (2.212(4), 2.216(4) and 2.210(4) Å) than the other three bonds involving the C(12), C(14) and C(15) carbon atoms (2.198(4), 2.189(5) and 2.190(4) Å). The average Ru–C distance is 2.202 Å, whereas the distance between the ruthenium atom and the centroid of the ring is 1.685 Å at the axis $x = 0.4391$, $y = 0.2239$ and $z = 0.1377$. These bond lengths are closely related to those in other reported

complexes [27]. The Ru–N bond lengths involving 3-methylpyrazole are 2.116(3) and 2.123(3) Å, respectively, well in accord with the literature values [29]. The Ru–Cl bond length is 2.3979(10) Å, which is within the usual range of Ru–Cl bond distances (2.39 Å) [31]. The geometry of the complex is octahedral with a piano-stool structure, and is marked by the nearly 90° value for the bond angles between the non-hexamethylbenzene ligands N(31)–Ru–N(21) (88.06(13°)), N(31)–Ru–Cl (85.34 (9°)), and N(21)–Ru–Cl (85.80(10°)) at the metal centre [32].

The molecular geometries of the dimeric cationic complexes **5c** and **5e**, which crystallize in the monoclinic and triclinic space groups $P2_1/n$ and $P\bar{1}$, are shown in Figs. 3 and 4. The ruthenium atom is π-bonded to the hexamethylbenzene ligand with the distances between ruthenium and the centroid of the six membered hexamethylbenzene rings equal to 1.684 Å and 1.669 Å, falling within the range found in other hexamethylbenzene ruthenium complexes [33]. An interesting feature of these crystal structures is their centrosymmetry, i.e., the two monomers are related to each other by an inversion center (Ci). In the case of complex **5e**, however, two isomers A and B exist in the solid state, both being centrosymmetric. In isomer A, the phenyl ring and the pyrazole ring attached to it are coplanner, but in isomer B they are slightly twisted with respect to each other. The isomer B is represented in Fig. 4. The monomers of complexes A and B are mirror images of each other (isomers) due to the different bond lengths between the Ru atom and two Cl atoms (i.e., Ru(A)–Cl(A) are 2.423(3) and 2.448(3) Å), and thus, different bond strengths, it is possible to break dimer A and B into monomers (Fig. 5). In solution, though, the two isomers are indistinguishable due to free rotation.

The Ru–N bond lengths in both the complexes (2.107(2)) Å for complex **5c**, and 2.101(7) Å for complex **5e** are comparable to that of Ru–N bond lengths in other related complexes [34]. The Ru–Cl bond lengths are 2.4390 Å (in **5c**) and 2.422(3) Å (in **5e**), which are within the range observed in reported complexes [35].

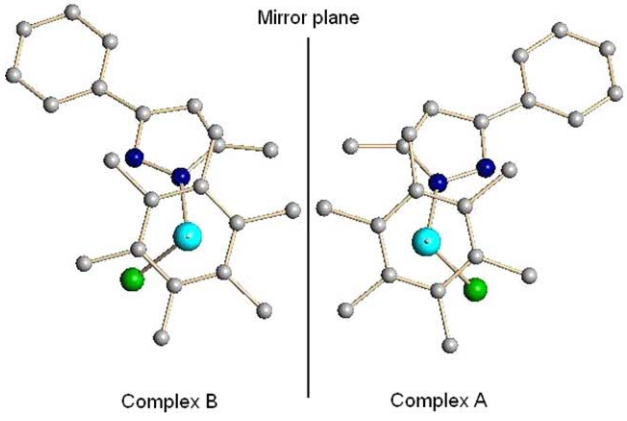

Fig. 5. Mirror images of the monomers of complexes A and B of the dimeric complex **5e**.

7. Conclusions

It is interesting to observe the differences between the two complexes **1** and **2**, where complex **1** gives the amidine complexes, while complex **2** gives disubstituted pyrazole complexes and chloro bridged pyrazole complexes depend on the bulkiness of the ligand. With increase in the ligand bulk, one can isolate the chloro bridged disubstituted pyrazole complexes from complex **2**. This is a clear indication that the steric factors of the ligands play a major role in the formation of these complexes.

Acknowledgements

K.M.R. and P.G. thank the Sophisticated Instruments Facility (SIF), Indian Institute of Science, Bangalore, for providing the NMR facility. We thank Prof. R.H. Duncan Lyngdoh for help in preparing the manuscript. We also thank for the referees for helpful suggestions.

Appendix A. Supplementary material

Crystallographic data for the structural analysis have been deposited at the Cambridge Crystallographic Data Centre (CCDC), CCDC No. **236402** for complex **5b**, CCDC No. **236403** for complex **5c,** and CCDC No. **236404** for complex **5e**. Copies of this information may be obtained free of charge from the director, CCDC, 12 Union Road, Cambridge, CB2 1EZ, UK (fax: +44-1223-336033; e-mail: deposit@ccdc.cam.ac.uk or www: http://www.ccdc.cam.ac.uk). Supplementary data associated with this article can be found, in the online version at doi:10.1016/j.jorganchem.2004.07.036.

References

[1] C.S. Slone, D.A. Weinberger, C.A. Mirkin, Prog. Inorg. Chem. 48 (1999) 233.
[2] (a) P. Jutzi, M.O. Kristen, B. Neumann, H.-G. Stammler, Organometallics 13 (1994) 3584;
(b) A. Baretta, K.S. Chong, F. Geoffrey, N. Cloke, A. Feigenbaum, M.L.H. Green, J. Chem. Soc., Dalton Trans. (1983) 861;
(c) P. Julzi, T. Redeker, Eur. J. Inorg. Chem. (1998) 663;
(d) M.S. Blais, J.C.W. Chien, M.D. Rausch, Organometallics 17 (1998) 3775;
(e) P. Jutzi, M.O. Kristen, J. Dahlhaus, B. Neumann, H.-G. Stammler, Organometallics 12 (1993) 2980;
(f) D.B. Grotjahn, C. Joubran, D. Combs, D.C. Brune, J. Am. Chem. Soc. 120 (1998) 11814;

(g) T.-F. Wang, C.-C. Hwu, C.-W. Tsai, Y.-S. Wen, Organometallics 17 (1998) 131;
(h) T.-F. Wang, C.-C. Hwu, C.W. Tsai, Y.S. Wen, J. Chem. Soc., Dalton Trans. (1998) 2901.

[3] (a) S.D.R. Christie, K.W. Man, R.J. Whitby, A.M.Z. Slawin, Organometallics 18 (1999) 348;
(b) D. Deng, C. Oian, G. Wu, P. Zheng, J. Chem. Soc., Chem Commun. (1990) 880;
(c) A.A.H. Vander Zeijden, C. Mattheis, R. Frahlich, Organometallics 16 (1997) 2651;
(d) A.A.H. Vander Zeijden, C. Mattheis, R. Frahlich, F. Zippel, Inorg. Chem. 36 (1997) 4444.

[4] (a) I. Lee, F. Dahan, A. Maisonnat, R. Poilblane, Organometallics 13 (1994) 2743;
(b) L. Lefort, T.W. Crane, M.D. Farwell, D.M. Baruch, J.A. Kaeuper, R.J. Lachicotte, W.D. Jones, Organometallics 17 (1998) 3889;
(c) L.P. Barthel Rosa, V.J. Catalono, K. Maitra, J.H. Nelson, Organometallics 15 (1996) 3924.

[5] (a) S.G. Davies, J.P. Mc Nally, A.J. Smallridge, Adv. Organomet. Chem. 30 (1991) 1 (and references therein);
(b) M.A. Bennett, K. Khan, E. Wenger, Comprehensive Organometallic Chemistry, Elsevier, Oxford, 1995 (and references cited therein);
(c) B.M. Trost, J.A. Marting, R.J. Kulawiec, A.F. Indoles, J. Am. Chem. Soc. 115 (1993) 10402;
(d) P. Pertici, V. Ballantini, P. Salvadori, M.A. Bennett, Organometallics 14 (1995) 2565;
(e) M.A. Harerov, F. Urberos, B. Chadred, Organometallics 12 (1993) 95.

[6] B. Therrien, T.R. Ward, Angew. Chem., Int. Ed. Engl. 38 (1999) 405.

[7] (a) P. Crochet, M.A. Fernandez-Zumel, C. Beauquis, J. Gimeno, Inorg. Chim. Acta 356 (2003) 114;
(b) K.Y. Ghebreyessus, J.H. Nelson, J. Organomet. Chem. 669 (2003) 48;
(c) V. Ritleng, R. Bertani, M. Pfeffer, C. Sirlin, J. Hirschinger, Inorg. Chem. 40 (2001) 5117;
(d) C.A. Merlic, M.E. Pauly, J. Am. Chem. Soc. 18 (1996) 11319;
(e) Z. Kabouche, C. Braneau, P.H. Dixneuf, Tetrahedron Lett. 32 (1991) 5359;
(f) K. Philippot, D. Devanne, P.H. Dixneuf, J. Chem. Soc., Chem Commun. (1990) 1199;
(g) H. Nagashima, H. Kondo, T. Hayashida, Y. Yamaguchi, M. Gondo, S. Masuda, K. Miyazaki, K. Matsubara, K.K. Kirchner, Coord. Chem. Rev. 245 (2003) 177.

[8] (a) R. Aird, J. Cummings, A. Ritchie, M. Muir, R. Morris, H. Chen, P.J. Sadler, D.I. Jodrell, Brit. J. Cancer 86 (2002) 1652;
(b) L.A. Hweham, E.L.S. Cheu, B.O. Patrick, B.R. James, Inorg. Chim Acta 352 (2003) 238.

[9] (a) C.S. Allardyce, P.J. Dyson, D.J. Ellis, P.A. Salter, R. Scopelliti, J. Organomet. Chem. 668 (2003) 35;
(b) H. Harvath, G. Laurency, A. Katho, J. Organomet. Chem. 689 (2004) 1036.

[10] (a) R.S. Garigipati, Tetrahedron Lett. 21 (1990) 1969;
(b) P. Oxley, M.W. Partridge, W.F. Short, J. Chem. Soc. (1947) 1110.

[11] (a) S. Derien, P.H. Dixneuf, J. Chem. Soc., Chem Commun. (1994) 2551;
(b) B.M. Trost, Angew. Chem., Int. Ed. Engl. 34 (1995) 259;
(c) J.W. Faller, C.J. Smart, Tetrahedron Lett. 30 (1989) 1189.

[12] C.S. Chin, D. Chong, B. Lee, H. Jeong, G. Won, Y. Do, Y.J. Park, Organometallics 19 (2000) 638 and references therein.

[13] C.J. Jones, J.A. McCleverty, A.S. Rothin, J. Chem. Soc., Dalton Trans (1986) 109.

[14] M.R. Kollipara, P. Sarkhel, S. Chakraborty, R. Lalrempuia, J. Coord. Chem. 56 (2003) 1085.

[15] (a) J. Lopez, A. Santos, A. Romero, J. Organomet. Chem 443 (1993) 221;
(b) M.A. Cinellu, S. Stoccoro, G. Minghetti, A.L. Bandini, G. Banditelli, B. Bovio, J. Organomet. Chem. 372 (1989) 311;
(c) G.D. Gracey, S.J. Rettig, A. Storr, J. Trotter, Can. J. Chem. 65 (1987) 2469;
(d) M.O. Albers, S. Francesca, A. Crosby, D.C. Liles, D.J. Robinson, A. Shaver, E. Wilkinson, A. Shaver, E. Singleton, Organometallics 6 (1987) 2014.

[16] (a) G. Süss-Fink, M. Faure, T.R. Ward, Angew. Chem. 114 (2002) 105;
(b) G. Süss-Fink, M. Faure, T.R. Ward, Angew. Chem., Int. Ed. Engl. 41 (2002) 99.

[17] M. Faure, M. Jahncke, A. Neels, H. Stoeckli-Evans, G. Süss-Fink, Polyhedron 18 (1999) 2679.

[18] (a) D. Carmona, J. Ferrer, L.A. Oro, M.C. Apreda, C. Foces-Foces, F.H. Cano, J. Elguero, M.A.L. Jimeno, J. Chem. Soc., Dalton Trans. (1990) 1463;
(b) W. Klaui, E. Buchholz, Inorg. Chem. 27 (1988) 3500;
(c) Y. Yamamoto, Y. Simozuka, Y. Tsutsumi, K. Fuse, K. Kuge, Y. Sunada, K. Tatsumi, Inorg. Chim. Acta 357 (2004) 1270.

[19] M.A. Bennett, A.K. Smith, J. Chem. Soc., Dalton Trans (1974) 233.

[20] (a) M.A. Bennett, T.N. Huang, T.W. Matheson, A.K. Smith, Inorg. Synth. 21 (1982) 74;
(b) M.A. Bennett, T.W. Matheson, G.B. Robertson, A.K. Smith, P.A. Tucker, Inorg. Chem. 19 (1980) 1014.

[21] J. Elguero, E. Gonzalez, R. Jacquier, Bull. Soc. Chim. Fr. (1968) 707.

[22] D. Becke, J. Chem. Phys. 98 (1993) 5648.

[23] XRD Single crystal software; Bruker Analytical X-ray systems: Madison, USA, 2002.

[24] G.M. Sheldrick, SHELXS 86, Program for Crystal Structure Solution, University of Göttengen, Göttengen, Germany, 1986.

[25] M. Sheldrick, SHELXS 97, Program for Crystal Structure Refinement, University of Göttengen, Göttengen, Germany, 1997.

[26] C.K. Johnson, ORTEP – II: A Fortran thermal Ellipsoid plot program for crystal structure illustrations, ORNL –5138, 1976.

[27] R.Y.C. Shin, M.A. Bennett, L.Y. Goh, W. Chen, D.C.R. Hockless, W.K. Leong, K. Mashima, A.C. Willis, Inorg. Chem. 42 (2003) 96.

[28] (a) H. Nishiyama, M. Konno, K. Aoki, Organometallics 21 (2002) 2536;
(b) Y. Miyaki, T. Onishi, H. Kurosawa, Inorg. Chim. Acta 300–302 (2000) 369.

[29] C.D. Nunes, M. Pillinger, A. Hazell, J. Jepsen, T.M. Santos, J. Madureira, A.D. Lopes, I.S. Goncalves, Polyhedron 22 (2003) 2799.

[30] J.M. Malecki, J.O. Dzuegielewski, M. Jaworksa, R. Kruszynki, T.J. Bartczak, Polyhedron 23 (2003) 885.

[31] (a) R. Baldwin, M.A. Bennett, D.C.R. Hockless, P. Pertici, A. Verrazzani, G.U. Barretta, F. Marchetti, P. Salvadori, J. Chem. Soc., Dalton Trans (2002) 4488;
(b) R. Lalrempuia, M.R. Kollipara, Polyhedron 22 (2003) 3155.

[32] A. Singh, N. Singh, D.S. Pandey, J. Organomet. Chem. 642 (2002) 48.

[33] (a) F.B. McCormick, W.B. Gleason, Acta Cryst. C44 (1988) 603;
(b) G.C. Martin, G.J. Palenik, J.M. Boncella, Inorg. Chem. 29 (1990) 2027.

[34] (a) Y. Miyaki, T. Onishi, H. Kurosawa, Inorg. Chim. Acta 300–302 (2000) 369;
(b) V. Cadierno, J. Diez, S.E. Garcia-Garrido, S. Garcia-Granda, J. Gimeno, J. Chem. Soc., Dalton Trans (2002) 1465.

[35] Y. Yamamoto, H. Nakamura, J.-F. Ma, J. Organomet. Chem 640 (2001) 10.